Subradiant Bell States in Distant Atomic Arrays

P.-O. Guimond, A. Grankin, D. V. Vasilyev, B. Vermersch, and P. Zoller
Center for Quantum Physics, University of Innsbruck, Innsbruck A-6020, Austria
and Institute for Quantum Optics and Quantum Information, Austrian Academy of Sciences, Innsbruck A-6020, Austria

(Received 9 January 2019; published 5 March 2019)

We study collective "free-space" radiation properties of two distant single-layer arrays of quantum emitters as two-level atoms. We show that this system can support a long-lived Bell superposition state of atomic excitations exhibiting strong subradiance, which corresponds to a nonlocal excitation of the two arrays. We describe the preparation of these states and their application in quantum information as a resource of nonlocal entanglement, including deterministic quantum state transfer with high fidelity between the arrays representing quantum memories. We discuss experimental realizations using cold atoms in optical trap arrays with subwavelength spacing, and analyze the role of imperfections.

DOI: 10.1103/PhysRevLett.122.093601

Introduction.—Recent advances in preparing regular arrays of atoms with optical traps [1–4] offer new opportunities to engineer strong collective coupling between atoms and light, with applications in quantum information science. In particular, a single layer of atoms loaded into a regular 2D array with subwavelength spacing has been proposed as an atomic mirror with high reflectivity [5–9], as quantum memory with efficient storage and retrieval [10], and to implement topological quantum optics [11,12]; in addition, emission of single photons from bilayer atomic arrays can be engineered to be highly directional in free-space [13]. Moreover, single-layered atomic arrays have been shown to support *subradiant* collective excitations [14–16], which consist of excited superposition states of atoms decaying much slower than a single isolated excited atom, due to interference in spontaneous emission [17–23].

Here we show that the composite quantum system consisting of two distant single-layered arrays of atoms [cf. Figs. 1(a)–1(c)] can support an atomic Bell superposition state exhibiting strong subradiance. Remarkably, this nonradiating "dark" state is a *nonlocal* entangled state, i.e., a superposition state of a collective excitation living in the first *or* second array, where the two arrays can be separated by a distance L much larger than the transverse size $L_\perp$ of each individual array. This phenomenon relies on two ingredients. First, spontaneous emission from a collective atomic excitation in a single layer can be directional, with a proper phasing of the atomic dipoles, corresponding to light emission in both directions perpendicular to the atomic array, as in Fig. 1(a) [5]. Second, radiation from two distant atomic arrays can—provided the separation length L is commensurate with half the optical wavelength [upper panel in Fig. 1(c)]—lead to destructive interference of light emitted to the left and to the right of the two arrays, corresponding to a subradiant state; i.e., this dark state will show strongly suppressed radiative loss to the outside world. In contrast, the lower panel in Fig. 1(c) displays a "bright" (i.e., radiating) state due to constructive interference.

Below we will show that these nonlocal subradiant atomic superposition states can be prepared naturally in setups involving two—or more—atomic arrays, and provide a source of entanglement shared between the two atomic arrays, with applications for quantum networking [24]. In particular, quantum information can be exchanged between the arrays representing "local" quantum memories, in a *coherent* and *deterministic* process, with dark states acting as mediators.

Quantum optical model.—Our setup consists of two 2D arrays of $N = N_\perp \times N_\perp$ atomic emitters with lattice spacing $\delta_\perp$ and size $L_\perp \equiv N_\perp \delta_\perp$, separated by a distance L along z. Each atom has a ground and an excited state, $|g\rangle_{\boldsymbol{j}}$ and $|e\rangle_{\boldsymbol{j}}$, and is coupled to free-space modes of the radiation field via a dipole transition with frequency $\omega_0 = ck_0 = 2\pi c/\lambda_0$. Here the multi-index $\boldsymbol{j} = (\boldsymbol{j}_\perp, j_z)$, where $j_z = 1, 2$ labels the arrays, while $\boldsymbol{j}_\perp = (j_x, j_y)$ label the atoms within each array, with $1 \le j_x,\ j_y \le N_\perp$. Atomic positions are denoted by $\boldsymbol{r}_{\boldsymbol{j}} = (x_j, y_j, z_j)$. We start by studying the dynamics of a single excitation with wave function $|\psi(t)\rangle = \sum_{\boldsymbol{j}} c_{\boldsymbol{j}}(t)\sigma_{\boldsymbol{j}}^+|\mathcal{G}\rangle|0\rangle + \int d\boldsymbol{k}\sum_\lambda \psi_\lambda(\boldsymbol{k},t)|\mathcal{G}\rangle|\boldsymbol{k},\lambda\rangle$. Here $\sigma_{\boldsymbol{j}}^+ = |e\rangle_{\boldsymbol{j}}\langle g|$, $|\mathcal{G}\rangle = \otimes_{\boldsymbol{j}} |g\rangle_{\boldsymbol{j}}$, $|0\rangle$ is the photonic vacuum state and $|\boldsymbol{k},\lambda\rangle$ the state with a single photon with wave vector $\boldsymbol{k}$ and polarization λ. We extend our results below to states with multiple excitations.

The atomic dynamics, due to successive photon emissions and reabsorptions, is obtained by integrating out the dynamics of the radiation modes $\psi_\lambda(\boldsymbol{k},t)$ in a Born-Markov approximation. Assuming the field initially in the vacuum

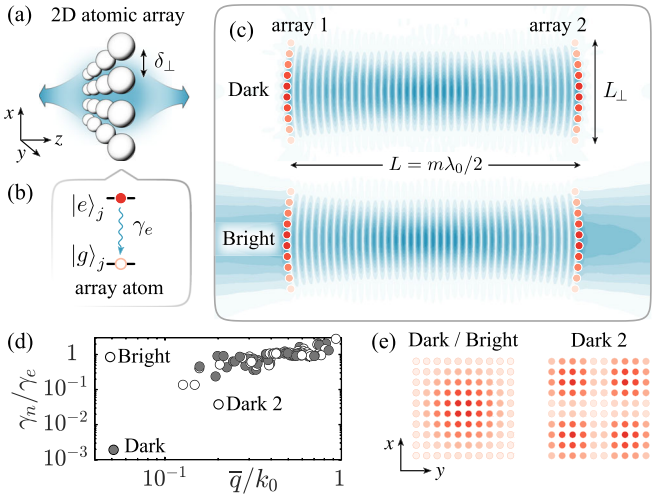

FIG. 1. Dark and bright states in two distant atomic arrays. (a) Sketch of a *single* 2D atomic array, with light emitted perpendicular to the atomic plane (corresponding to a bright, i.e., radiating state). (b) Two-level scheme. (c) Setup with two distant atomic arrays: we plot the electric field profile $|\boldsymbol{\psi}(\boldsymbol{r})|$ of photonic modes (blue) associated with the dark and bright states as excitations in the two arrays (red). (d) Decay rates γ_n as the imaginary part of eigenenergies of the non-Hermitian effective Hamiltonian $\mathcal{H}$ [Eq. (1)], in units of the single atom decay rate γ_e, ordered according to their quasimomentum $\bar{q}$ (see text). The white (black) color denotes even (odd) parity. A pair of dark and bright states are identified as the left-most dots. (e) Atomic wave function amplitudes in each array $|(v_n)_{\boldsymbol{j}_\perp}|$ associated with the dark and bright state. In (c)–(e) $\delta_\perp = 0.75\lambda_0$, $N_\perp = 10$, $L = 20\lambda_0$ (see text).

state $\psi_\lambda(\boldsymbol{k}, 0) = 0$, this yields $\dot{c}_j = -i\sum_{j'}\mathcal{H}_{jj'}c_{j'}$, where in a frame rotating with ω_0 [25–27],

$$\mathcal{H}_{jj'} \equiv -i(\gamma_e/2)\boldsymbol{p}^* \cdot \hat{\boldsymbol{G}}(\boldsymbol{r}_j - \boldsymbol{r}_{j'}) \cdot \boldsymbol{p} \tag{1}$$

is a non-Hermitian effective Hamiltonian, whose Hermitian part describes coherent exchanges of atomic excitations, while the non-Hermitian part corresponds to dissipation accounting for radiation of photons. Here γ_e is the spontaneous decay rate of each atom, and the dyadic Green's tensor $\hat{\boldsymbol{G}}(\boldsymbol{r})$, representing the electric field at position $\boldsymbol{r}$ generated by a dipole located at the origin, is the solution of $\boldsymbol{\nabla}\times\boldsymbol{\nabla}\times\hat{\boldsymbol{G}}(\boldsymbol{r}) - k_0^2\hat{\boldsymbol{G}}(\boldsymbol{r}) + (6\pi i/k_0)\delta(\boldsymbol{r}) = 0$ with $\hat{\boldsymbol{G}}(\boldsymbol{0}) \equiv \mathbb{1}$ accounting for independent single-atom decay (see details in Ref. [28]). The atomic transition polarization $\boldsymbol{p}$ is taken circular, with z as quantization axis.

Dark and bright eigenstates.—The dynamics of atomic excitations, including their radiative properties, can be understood by studying the spectrum of $\mathcal{H}$. Denoting its eigenvalues as $\epsilon_n = \Delta_n - i\gamma_n/2$ (with $n = 1, \ldots, 2N$), Δ_n is interpreted as the self-energy of the collective atomic excitation given by the corresponding eigenstate c_n, while γ_n is its spontaneous emission rate. In particular, an eigenstate is *subradiant* (or dark) if spontaneous emission occurs with a rate suppressed below the single-atom decay rate γ_e. In view of the mirror symmetry of the system, all eigenstates have a definite parity; i.e., they can be written as $(c_n)_{(\boldsymbol{j}_\perp,1)} = p_n(c_n)_{(\boldsymbol{j}_\perp,2)} \equiv (v_n)_{\boldsymbol{j}_\perp}/\sqrt{2}$, with parity $p_n = \pm 1$.

In Fig. 1(d) we plot the decay rates [for the setup of Fig. 1(c)], with parameters chosen as explained below. One of the eigenstates is remarkably subradiant, with a decay rate of $\gamma_d \sim 10^{-3}\gamma_e$. We also represent the mean absolute value of the transverse quasimomentum $\bar{q}$, which is obtained from the discrete Fourier transform of the corresponding eigenvectors $(\tilde{v}_n)_{\boldsymbol{q}} = \sum_{\boldsymbol{j}_\perp}(v_n)_{\boldsymbol{j}_\perp}e^{i\delta_\perp \boldsymbol{j}_\perp\cdot\boldsymbol{q}}/\sqrt{N}$ as $\bar{q} = \sum_{\boldsymbol{q}}|(\tilde{v}_n)_{\boldsymbol{q}}|^2|\boldsymbol{q}|$, with discrete quasimomentum $\boldsymbol{q} = (q_x, q_y)$, where $q_{x,y} = -\pi/\delta_\perp + 2\pi n_{x,y}/L_\perp$ ($n_{x,y} = 0, 1, \ldots, N_\perp - 1$). Two states have a distinctly low quasimomentum $\bar{q} \ll k_0$: the dark state, as well as a bright state, which radiates photons with a rate γ_b comparable to γ_e. We contrast our dark states with the $\bar{q} > k_0$ subradiant states in single layer setups, studied, e.g., in Refs. [16,20]. In Fig. 1(e) we show the probability amplitude of the eigenvectors $|(v_n)_{\boldsymbol{j}_\perp}|$ for the two states with lowest decay rates [28].

This pair of dark and bright states can be understood by considering first the situation where the arrays are infinite ($N_\perp \to \infty$), and the eigenstates are plane waves $(v_n)_{\boldsymbol{j}_\perp} = e^{i\delta_\perp \boldsymbol{j}_\perp\cdot\boldsymbol{q}_n}/\sqrt{N}$ with continuous quasimomentum $\boldsymbol{q}_n$. We now make two assumptions: First, the lattice spacing satisfies $\delta_\perp < \lambda_0$. Under this condition, we obtain, provided $|\boldsymbol{q}_n| \leq 2\pi/\delta_\perp - k_0$ [28],

$$\gamma_n = \Gamma[1 + p_n\cos(k_z L)]\frac{k_z^2 + |\boldsymbol{q}_n|^2/2}{k_0 q_z}, \tag{2}$$

with $\Gamma = 3\pi\gamma_e/(k_0\delta_\perp)^2$, $k_z = \sqrt{k_0^2 - |\boldsymbol{q}_n|^2}$. Considering in particular the symmetric ($p_n = 1$) and antisymmetric ($p_n = -1$) eigenstates with $\boldsymbol{q}_n = \boldsymbol{0}$, we obtain a pair of states with decay rates $\gamma_{s/a} = \Gamma[1 \pm \cos(k_0 L)]$. Similarly, their self-energies are $\Delta_{s/a} = \pm(\Gamma/2)\sin(k_0 L) + \Delta_d$, as depicted in Fig. 2(b), where Δ_d is a collective Lamb shift evaluated numerically. Our second assumption is that $k_0 L = m\pi$ with integer m, so that either γ_s or γ_a vanishes due to interference in the emission of the two arrays, while the other reduces to $\gamma_b = 2\Gamma$. The corresponding Bell states,

$$|\psi_{d/b}\rangle = \frac{1}{\sqrt{2N}}\sum_{\boldsymbol{j}_\perp}[\sigma^+_{(\boldsymbol{j}_\perp,1)} \mp (-1)^m\sigma^+_{(\boldsymbol{j}_\perp,2)}]|\mathcal{G}\rangle, \tag{3}$$

are thus, respectively, dark and bright.

For finite-sized arrays, the eigenstates $(v_n)_{\boldsymbol{j}_\perp}$ are confined, which has two consequences yielding a finite decay rate γ_d for the dark state. First, photon emission in the transverse directions is not perfectly cancelled. Second, photons emitted along z have a finite spread of transverse

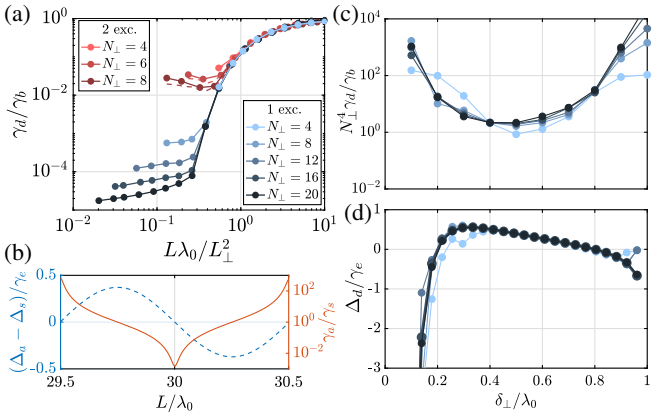

FIG. 2. Dark and bright state properties. (a) Ratio of dark and bright states decay rates for 1 (blue) and 2 (red) excitations, with $\delta_\perp = \lambda_0/2$ and $L = m\lambda_0/2$ with integer m. (b) Collective frequency shifts (dashed blue) and decay rates (red) of parity-symmetric (s) and antisymmetric (a) single-excitation states, with $\delta_\perp = 0.8\lambda_0$ and $N_\perp = 12$. (c) Dark and bright state decay rates, and (d) collective frequency shift of the dark state, for $L = 2\lambda_0$, $\delta_\perp = \lambda_0/2$, and $N_\perp$ as in (a) for 1 excitation.

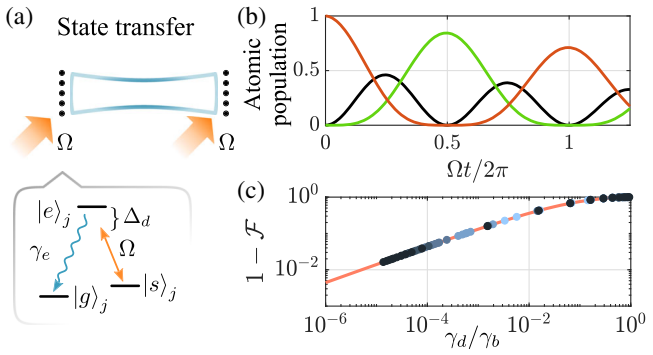

FIG. 3. Quantum state transfer between local quantum memories. (a) Sketch and atomic Λ-level structure for coupling quantum memories. A weak homogeneous field Ω, resonant with the collective atomic shift Δ_d, drives the $|e\rangle \to |s\rangle$ transition. (b) Temporal evolution of the atomic populations for the initial state $S_1^+|\mathcal{G}\rangle$, with $N_\perp = 12$, $L = 30\lambda_0$, $\delta_\perp = 0.8\lambda_0$. Red (green): number of atoms in state $|s\rangle$ in the first (second) array. Black: total number of atoms in state $|e\rangle$. (c) Infidelity for quantum state transfer as function of dark and bright state decay rates. Blue dots: parameters of Fig. 2(a) for 1 excitation. Red curve: Eq. (5).

momentum, and thus diffract when propagating between the two arrays, thereby hindering the interference of emission. This can be mitigated by curving the arrays according to the phase profile of a Gaussian mode $\mathcal{E}(\boldsymbol{r})$ propagating along z [as shown in Fig. 1(c)], in analogy to the mirrors of an optical cavity. As represented in Fig. 1(e), the spatial distribution of the dark state (as well as the bright state) is then $(v_d)_{\boldsymbol{j}_\perp} \propto \mathcal{E}(\boldsymbol{r}_{(\boldsymbol{j}_\perp,1)})$ [29]. Alternatively, one can add optical elements between the arrays, such as lenses or fibers.

The spatial profile of the electric field, generated by (virtual) photon exchanges between the atomic dipoles in the dark state, reads $\boldsymbol{\psi}(\boldsymbol{r}) \sim \sum_{\boldsymbol{j}} c_{\boldsymbol{j}} \hat{\boldsymbol{G}}(\boldsymbol{r} - \boldsymbol{r}_{\boldsymbol{j}}) \cdot \boldsymbol{p}$, and forms a standing wave [see Fig. 1(c)]. We emphasize that—although the system resembles a cavity with each array acting as a mirror—we are interested here in the quantum state of the *atoms*. More precisely, the ratio of atomic to photonic excitations in the dark state is given by $\Gamma L/(2c)$ with speed of light c [28], which is assumed negligible when integrating the field dynamics above, amounting to neglecting retardation effects in the atomic dynamics. This is in analogy to atomic cavities built from strings of atoms coupled to a 1D waveguide [30,31].

We now discuss how the geometric parameters ($N_\perp$, L, $\delta_\perp$) affect the spectral properties of the system. In Fig. 2(a) we show the scaling of γ_d/γ_b as the relevant figure of merit, with the waist of $\mathcal{E}(\boldsymbol{r})$ minimizing this ratio. Low ratios can be achieved for $L \lesssim L_\perp^2/\lambda_0$, a condition set by the diffraction limit; i.e., the spot size of the Gaussian mode must be smaller than the surface of the arrays. Remarkably, this condition allows us to achieve strong subradiance even when the characteristic size of each array $L_\perp$ is much smaller than their separation L; i.e., the subradiant state is nonlocal. As an example, for $N_\perp = 20$ and $\delta_\perp = 0.8\lambda_0$ (i.e., $L_\perp = 16\lambda_0$), we obtain $\gamma_d/\gamma_b \sim 10^{-2}$ for $L \sim 130\lambda_0$.

In Fig. 2(b) we observe that the interference mechanism is quite sensitive to the separation between arrays, as small deviations of L compared to λ_0 will greatly increase the decay rate γ_d [see Eq. (2)]. In Fig. 2(c) we show the effect of the lattice spacing on the saturation value of Fig. 2(a) for small L. The ratio of dark to bright state decay rates is minimal for $\delta_\perp = \lambda_0/2$, for which the emission in transverse directions is best cancelled, and scales with the atom number as $\gamma_d/\gamma_b \sim 1/N_\perp^4$. The collective shift Δ_d on the other hand is typically of the order of γ_e [cf. Fig. 2(d)]. It can be positive or negative depending on $\delta_\perp$, and vanishes around $\delta_\perp = 0.2\lambda_0$ and $\delta_\perp = 0.8\lambda_0$ (see also Ref. [9]).

Dark state preparation and quantum state transfer.—In order to prepare the atoms in the dark state, we consider the setup represented in Fig. 3(a), where the atomic level structure now includes a third state $|s\rangle$. We assume that the system is initially in a superposition state of the first array $S_1^+|\mathcal{G}\rangle$, with $S_1^+ = \sum_{\boldsymbol{j}_\perp} (v_d)_{\boldsymbol{j}_\perp} |s\rangle_{(\boldsymbol{j}_\perp,1)}\langle g|$. This could be realized, for instance, using laser-dressed Rydberg-Rydberg interactions [13,32], or single photon pulses [28]. Moreover, we assume a coherent field drives the $|s\rangle \to |e\rangle$ transition in the first array with Rabi frequency Ω, resonantly with the collective shift Δ_d. The atoms are thus driven from state $S_1^+|\mathcal{G}\rangle$ to a superposition of dark and bright states $\sum_{\boldsymbol{j}_\perp} (v_d)_{\boldsymbol{j}_\perp} \sigma^+_{(\boldsymbol{j}_\perp,1)}|\mathcal{G}\rangle = (1/\sqrt{2})(\sigma_b^+ + \sigma_d^+)|\mathcal{G}\rangle$, where the operators $\sigma^+_{d/b} \equiv \sum_{\boldsymbol{j}_\perp} (v_d)_{\boldsymbol{j}_\perp} (\sigma^+_{(\boldsymbol{j}_\perp,1)} \mp [-1]^m \sigma^+_{(\boldsymbol{j}_\perp,2)})/\sqrt{2}$ create a dark and bright atomic excitation. The decay rate of bright excitations can be orders of magnitude larger than for dark excitations, such that their contribution to the dynamics is vastly different. If $\gamma_b \gg \Omega$,

the bright mode can be adiabatically eliminated, and contributes an effective loss with rate Ω^2/γ_b, which can vanish in the spirit of a quantum Zeno effect. On the other hand, if $\Omega \gg \gamma_d$, the dynamics will yield oscillations between the initial state and the nonlocal dark state.

This mechanism can be exploited for quantum state transfer between the two arrays. Here, an initial qubit superposition state in the first array $|\psi_i\rangle = c_g|\mathcal{G}\rangle + c_s S_1^+|\mathcal{G}\rangle$ (with $|c_g|^2 + |c_s|^2 = 1$) is transferred deterministically to the second array. That is, we realize the process $|\psi_i\rangle \to |\psi_f\rangle = c_g|\mathcal{G}\rangle + c_s S_2^+|\mathcal{G}\rangle$, where $S_2^+ = \sum_{\boldsymbol{j}_\perp} (v_d)_{\boldsymbol{j}_\perp} |s\rangle_{(\boldsymbol{j}_\perp,2)}\langle g|$, with high fidelity $\mathcal{F} \approx 1$ [33]. By driving atoms in both arrays with Rabi frequency Ω, the state $S_2^+|\mathcal{G}\rangle$ is coupled to the opposite superposition $\sum_{\boldsymbol{j}_\perp}(v_d)_{\boldsymbol{j}_\perp} \sigma^+_{(\boldsymbol{j}_\perp,2)}|\mathcal{G}\rangle = (1/\sqrt{2})(\sigma_b^+ - \sigma_d^+)|\mathcal{G}\rangle$, and we can write an effective model, where the system is described by four excitation modes: two local modes, with creation operators S_1^+ and S_2^+, which represent quantum memories in $|\psi_i\rangle$ and $|\psi_f\rangle$; and two nonlocal bright and dark modes, with creation operators σ_b^+ and σ_d^+, connecting the two memories. The dynamics can then be described by a Lindblad master equation for the density matrix of the atoms ρ, as $\dot{\rho} = -i[H_{\text{eff}}, \rho] + \gamma_d \mathcal{D}[\sigma_d^-]\rho + \gamma_b \mathcal{D}[\sigma_b^-]\rho$, where $\mathcal{D}[a]\rho \equiv a\rho a^\dagger - (1/2)(a^\dagger a \rho + \rho a^\dagger a)$, and with an effective Hamiltonian

$$H_{\text{eff}} = \frac{\Omega}{\sqrt{2}}[\sigma_b^+(S_1^- + S_2^-) + \sigma_d^+(S_1^- - S_2^-)] + \text{H.c.} \quad (4)$$

The evolution of the system is shown in Fig. 3(b), demonstrating transfer at time $t = \pi/\Omega$ [34]. We emphasize that our protocol does not require tailoring the temporal shape of exchanged photons, in contrast to deterministic quantum state transfer protocols with "flying" photonic qubits [13,35]. Figure 3(c) represents in red the optimal achievable fidelity for given $\gamma_{d,b}$, which reads

$$\mathcal{F} \approx e^{-\pi\sqrt{2\gamma_d/\gamma_b}}, \quad (5)$$

showing the requirement $\gamma_b \gg \gamma_d$. The blue dots represent simulations for atomic arrays with the parameters of Fig. 2(a), with the optimal drive given by $\Omega = \sqrt{\gamma_d\gamma_b/8}$ [28]. As noted above, our treatment neglects effects of retardation in atomic dynamics; Eq. (5) remains, however, valid even for large delay times, although at the cost of a slowdown of the dynamics [28].

Probing the dark state.—The existence of the dark state can be detected in the reflection of an external laser (see details in Ref. [28]). We consider here a weak probing field with frequency $\omega_0 + \Delta_d$, propagating along z in the Gaussian mode $\mathcal{E}(\boldsymbol{r})$, and driving atoms prepared in the ground state $|\mathcal{G}\rangle$. Assuming the transition frequency of the atoms in each array is additionally detuned, by Δ for atoms in the first array and either Δ or $-\Delta$ for the second array, the dark and bright states are then revealed in the width of the resonance peak of the reflectivity $R(\Delta)$. We obtain $R = (\gamma_b - \gamma_d)^2/(\gamma_b^2 + 4\Delta^2)$ for symmetric detuning, and $R = (\gamma_b - \gamma_d)^2/(\gamma_b + 4\Delta^2/\gamma_d)^2$ for opposite detuning, which both have a peak at $\Delta = 0$ [28]; the widths of these peaks are given by γ_b and $\sim\sqrt{\gamma_d\gamma_b}$, respectively, allowing for a direct probing of the dark state lifetime.

Experimental considerations.—The level structure can be implemented in neutral atoms using, for instance, stretched states of ^{87}Rb for $|g\rangle = |5S_{1/2}, F = 2, m_F = 2\rangle$, and $|e\rangle = |5P_{3/2}, F = 3, m_F = 3\rangle$, along with a strong magnetic field to eliminate other hyperfine states from the dynamics. The level $|s\rangle$ needs to be coherently coupled to the excited state, while avoiding spontaneous decay from $|e\rangle$ to $|s\rangle$. This could be realized, for example, using a Rydberg state $|s\rangle = |nS_{1/2}, m = 1/2\rangle$, with higher energy [10], or another ground state $|s\rangle = |5S_{1/2}, F = 1, m_F = 1\rangle$, coupled to $|e\rangle$ via a two-photon transition [36]. Alternatively, one can use for the optical transition atoms with a $J = 0 \to J = 1$ transition, e.g., ^{88}Sr; while this introduces three excited states with orthogonal dipole matrix elements, our results for dark and bright state decay rates remain qualitatively similar [28].

The atomic trap is characterized by a finite temperature and Lamb-Dicke parameter η [37]. The resulting spread of the atomic wave function yields a renormalization of the decay rates as $\gamma_{d/b} \to \gamma_{d/b}[1 - \eta^2(2n_{\text{th}} + 1)] + \gamma_e\eta^2(2n_{\text{th}} + 1)$ [28], where n_{th} is the thermal occupation number of trap states, and we assumed $\eta\sqrt{2n_{\text{th}} + 1} \ll 1$ and $\gamma_e\eta\sqrt{2n_{\text{th}} + 1} \ll \omega_\nu$, with ω_ν the atomic motional frequency. We thus need $\eta^2(2n_{\text{th}} + 1) \lesssim \gamma_d/\gamma_e$. The effect of missing atoms is similar [28]; for a defect probability p, we find $\gamma_{d/b} \to \gamma_{d/b}(1 - p) + \gamma_e p + O(p^2)$; i.e., we require $p \lesssim \gamma_d/\gamma_e$.

Multiple excitations.—For states with multiple excitations, the dynamics can be studied again by analyzing the spectral properties of the non-hermitian effective Hamiltonian, which now takes the form $H_{\text{dip}} = \sum_{\boldsymbol{j}\boldsymbol{j}'} \mathcal{H}_{\boldsymbol{j}\boldsymbol{j}'} \sigma_{\boldsymbol{j}}^+ \sigma_{\boldsymbol{j}'}^-$ [28]. Since each atom cannot be excited more than once, the doubly excited state $(\sigma_d^+)^2|\mathcal{G}\rangle$ cannot be an exact eigenstate of H_{dip}. An analytical expression for the resulting decay rates can, however, be obtained by treating the nonlinearity as perturbation, where each excitation effectively acts as a defect for the other, with the "defect" probability p identified as the inverse participation ratio $p = \sum_{\boldsymbol{j}_\perp} |(v_d)_{\boldsymbol{j}_\perp}|^4$ (see Ref. [28]). In Fig. 2(a) we show in red, for the eigenstate closest to $(\sigma_d^+)^2|\mathcal{G}\rangle$, the ratio of the decay rate per excitation $\gamma_d^{(2)}$ and γ_b, which is well captured by this analytical approximation (dashed red curves).

For large $N_\perp$, we thus expect $\gamma_d^{(2)} \sim \gamma_e/N_\perp^2$, since $(v_d)_{\boldsymbol{j}_\perp} \sim 1/N_\perp$. Two regimes can then be explored. First,

for γ_d, $\gamma_d^{(2)} \ll \gamma_b$ the system becomes effectively almost linear, and, in particular, the protocol for quantum state transfer above remains valid, with the replacement $\gamma_d \to \gamma_d^{(2)}$. This can be used to transfer states with more than one excitation, e.g., quantum error correcting states such as cat or binomial states [38], allowing in principle to reach fidelities beyond Eq. (5). Second, if $\gamma_d \ll \gamma_d^{(2)}$, γ_b, excitations of radiating two-excitation states can be adiabatically eliminated, exploiting again the quantum Zeno effect. This mechanism can be used to effectively block the transfer from the memories to the dark state, and thereby can operate as a controlled-phase gate [39]. Moreover, by the same principle, weakly driving the optical transition of atoms in one of the arrays generates Rabi oscillations between $|\mathcal{G}\rangle$ and $\sigma_d^+|\mathcal{G}\rangle$ as a two-level system, which can also be used to prepare the system in the dark state, e.g., for entanglement generation between memories, or as single-photon source.

Conclusion.—We have shown that distant single-layered arrays of two-level atoms can support subradiant (long-lived) states as collective excitations in the form of Bell superpositions. Our setup constitutes a building block for a modular quantum architecture, where quantum information, stored and processed in atomic arrays, is exchanged via dark modes. Moreover, the separation between arrays can be drastically increased by adding lenses or optical fibers to mediate photons between the arrays, although at the cost of adding decoherence channels. While we discussed here implementations with atoms in optical lattices, our results remain valid for other types of emitters, including, for instance, in solid-state platforms such as color centers in diamond [40], quantum dots [41], or monolayers of transition metal dichalcogenides [42].

We thank A. Asenjo-Garcia, D. Chang, F. Robicheaux, J. Ruostekoski, and M. Saffman for comments on the manuscript. This work was supported by the Army Research Laboratory Center for Distributed Quantum Information via the project SciNet, the ERC Synergy Grant UQUAM, and the SFB FoQuS (FWF Project No. F4016-N23).

[1] B. J. Lester, N. Luick, A. M. Kaufman, C. M. Reynolds, and C. A. Regal, Phys. Rev. Lett. **115**, 073003 (2015).
[2] T. Xia, M. Lichtman, K. Maller, A. W. Carr, M. J. Piotrowicz, L. Isenhower, and M. Saffman, Phys. Rev. Lett. **114**, 100503 (2015).
[3] M. Endres, H. Bernien, A. Keesling, H. Levine, E. R. Anschuetz, A. Krajenbrink, C. Senko, V. Vuletic, M. Greiner, and M. D. Lukin, Science **354**, 1024 (2016).
[4] D. Barredo, S. de Léséleuc, V. Lienhard, T. Lahaye, and A. Browaeys, Science **354**, 1021 (2016).
[5] F. J. García de Abajo, Rev. Mod. Phys. **79**, 1267 (2007).
[6] S. D. Jenkins and J. Ruostekoski, Phys. Rev. Lett. **111**, 147401 (2013).
[7] R. J. Bettles, S. A. Gardiner, and C. S. Adams, Phys. Rev. Lett. **116**, 103602 (2016).
[8] S. D. Jenkins, J. Ruostekoski, N. Papasimakis, S. Savo, and N. I. Zheludev, Phys. Rev. Lett. **119**, 053901 (2017).
[9] E. Shahmoon, D. S. Wild, M. D. Lukin, and S. F. Yelin, Phys. Rev. Lett. **118**, 113601 (2017).
[10] M. T. Manzoni, M. Moreno-Cardoner, A. Asenjo-Garcia, J. V. Porto, A. V. Gorshkov, and D. E. Chang, New J. Phys. **20**, 083048 (2018).
[11] J. Perczel, J. Borregaard, D. E. Chang, H. Pichler, S. F. Yelin, P. Zoller, and M. D. Lukin, Phys. Rev. Lett. **119**, 023603 (2017).
[12] R. J. Bettles, J. Minář, C. S. Adams, I. Lesanovsky, and B. Olmos, Phys. Rev. A **96**, 041603 (2017).
[13] A. Grankin, P. O. Guimond, D. V. Vasilyev, B. Vermersch, and P. Zoller, Phys. Rev. A **98**, 043825 (2018).
[14] G. Facchinetti, S. D. Jenkins, and J. Ruostekoski, Phys. Rev. Lett. **117**, 243601 (2016).
[15] D. Plankensteiner, C. Sommer, H. Ritsch, and C. Genes, Phys. Rev. Lett. **119**, 093601 (2017).
[16] A. Asenjo-Garcia, M. Moreno-Cardoner, A. Albrecht, H. J. Kimble, and D. E. Chang, Phys. Rev. X **7**, 031024 (2017).
[17] R. H. Dicke, Phys. Rev. **93**, 99 (1954).
[18] M. O. Scully, Phys. Rev. Lett. **115**, 243602 (2015).
[19] W. Guerin, M. O. Araújo, and R. Kaiser, Phys. Rev. Lett. **116**, 083601 (2016).
[20] R. T. Sutherland and F. Robicheaux, Phys. Rev. A **94**, 013847 (2016).
[21] H. H. Jen, M.-S. Chang, and Y.-C. Chen, Phys. Rev. A **94**, 013803 (2016).
[22] P. Solano, P. Barberis-Blostein, F. K. Fatemi, L. A. Orozco, and S. L. Rolston, Nat. Commun. **8**, 1857 (2017).
[23] M. Moreno-Cardoner, D. Plankensteiner, L. Ostermann, D. E. Chang, and H. Ritsch, arXiv:1901.10598.
[24] T. E. Northup and R. Blatt, Nat. Photonics **8**, 356 (2014).
[25] R. H. Lehmberg, Phys. Rev. A **2**, 883 (1970).
[26] D. F. V. James, Phys. Rev. A **47**, 1336 (1993).
[27] L. Novotny and B. Hecht, *Principles of Nano-Optics* (Cambridge University Press, Cambridge, England, 2006).
[28] See Supplemental Material at http://link.aps.org/supplemental/10.1103/PhysRevLett.122.093601 for more details.
[29] Analytical expressions are obtained below within a paraxial approximation.
[30] D. E. Chang, L. Jiang, A. V. Gorshkov, and H. J. Kimble, New J. Phys. **14**, 063003 (2012).
[31] P.-O. Guimond, A. Roulet, H. N. Le, and V. Scarani, Phys. Rev. A **93**, 023808 (2016).
[32] D. Petrosyan and K. Mølmer, Phys. Rev. Lett. **121**, 123605 (2018).
[33] We define the fidelity $\mathcal{F} \equiv \mathrm{Tr}[\rho(T)|\psi_f\rangle\langle\psi_f|]$, as the probability of successful transfer, with $\rho(T)$ the density matrix at the end of the protocol with $c_s = 1$.
[34] The protocol is terminated by switching off the laser drive.
[35] J. I. Cirac, P. Zoller, H. J. Kimble, and H. Mabuchi, Phys. Rev. Lett. **78**, 3221 (1997).
[36] D. Porras and J. I. Cirac, Phys. Rev. A **78**, 053816 (2008).

[37] A. D. Ludlow, M. M. Boyd, J. Ye, E. Peik, and P. O. Schmidt, Rev. Mod. Phys. **87**, 637 (2015).
[38] M. H. Michael, M. Silveri, R. T. Brierley, V. V. Albert, J. Salmilehto, L. Jiang, and S. M. Girvin, Phys. Rev. X **6**, 031006 (2016).
[39] D. Dzsotjan, A. S. Sørensen, and M. Fleischhauer, Phys. Rev. B **82**, 075427 (2010).
[40] M. W. Doherty, N. B. Manson, P. Delaney, F. Jelezko, J. Wrachtrup, and L. C. L. Hollenberg, Phys. Rep. **528**, 1 (2013).
[41] P. Lodahl, S. Mahmoodian, and S. Stobbe, Rev. Mod. Phys. **87**, 347 (2015).
[42] Y. Zhou, G. Scuri, J. Sung, R. J. Gelly, D. S. Wild, K. De Greve, A. Y. Joe, T. Taniguchi, K. Watanabe, P. Kim, M. D. Lukin, and Hongkun Park, arXiv:1901.08500.